Io Volcano Observer's (IVO) Integrated Approach to Optimizing System Design for Radiation Challenges.

Elena Adams,
Kenneth Hibbard, Elizabeth Turtle, Edward Reynolds, Brian Anderson, Chris Paranicas, Gabe Rogers, James McAdams, and David Roth

The Johns Hopkins University Applied Physics Laboratory
11100 Johns Hopkins Rd
Laurel, MD 20723-6099
240-228-7265
Elena.Adams@jhuapl.edu; Kenneth.Hibbard@ jhuapl.edu; Elizabeth.Turtle@jhuapl.edu; Edward.Reynolds@jhuapl.edu; Brian.Anderson@ jhuapl.edu; Chris. Paranicas@ jhuapl.edu; Gabe.Rogers@ jhuapl.edu; Jim.McAdams@jhuapl.edu; David.Roth@ jhuapl.edu

Alfred McEwen

Department of Planetary Sciences
Lunar and Planetary Laboratory
University of Arizona
Tucson, AZ 85721-0092
Mcewen@pirl.lpl.arizona.edu

Nicolas Thomas and Peter Wurz

Physikalisches Institut
University of Bern,
Bern CH-3012 Switzerland
Nicolas.Thomas @space.unibe.ch;
Peter.Wurz@space.unibe.ch

Phil Christensen

School of Earth and Space Exploration
Arizona State University
Tempe, AZ 85287-6305
Phil.Christensen @asu.edu

Martin Wieser

Swedish Institute of Space Physics IRF
Kiruna, 98128 Sweden
wieser@irf.se

James Janesick

Advanced Sensor Group
SRI Sarnoff Corporation
Huntington Beach, CA 92649
(cmosccd@aol.com).

Abstract - **One of the major challenges for a mission to the Jovian system is the radiation tolerance of the spacecraft (S/C) and the payload. Moreover, being able to achieve science observations with high signal to noise ratios (SNR), while passing through the high flux radiation zones, requires additional ingenuity on the part of the instrument provider. Consequently, the radiation mitigation is closely intertwined with the payload, spacecraft and trajectory design, and requires a systems-level approach. This paper presents a design for the *Io Volcano Observer (IVO)*, a Discovery mission concept that makes multiple close encounters with Io while orbiting Jupiter. The mission aims to answer key outstanding questions about Io, especially the nature of its intense active volcanism and the internal processes that drive it. The payload includes narrow-angle and wide-angle cameras (NAC and WAC), dual fluxgate magnetometers (FGM), a thermal mapper (ThM), dual ion and neutral mass spectrometers (INMS), and dual plasma ion analyzers (PIA). The radiation mitigation is implemented by drawing upon experiences from designs and studies for missions such as the *Radiation Belt Storm Probes* (*RBSP*) and *Jupiter Europa Orbiter* (*JEO*). At the core of the radiation mitigation is *IVO*'s inclined and highly elliptical orbit, which leads to rapid passes through the most intense radiation near Io, minimizing the total ionizing dose (177 krads behind 100 mils of Aluminum with radiation design margin (RDM) of 2 after 7 encounters). The payload and the spacecraft are designed specifically to accommodate the fast flyby velocities (e.g. the spacecraft is radioisotope powered, remaining small and agile without any flexible appendages). The science instruments, which collect the majority of the high-priority data when close to Io and thus near the peak flux, also have to mitigate transient noise in their detectors. The cameras use a combination of shielding and CMOS detectors with extremely fast readout to minimize noise. INMS microchannel plate detectors and PIA channel electron multipliers require additional shielding. The FGM is not sensitive to noise induced by energetic particles and the ThM microbolometer detector is nearly insensitive. Detailed SNR calculations are presented. To facilitate targeting agility, all of the spacecraft components are shielded separately since this approach is more mass efficient than using a radiation vault. *IVO* uses proven radiation-hardened parts (rated at 100 krad behind equivalent shielding of 280 mils of Aluminum with RDM of 2) and is expected to have ample mass margin to increase shielding if needed.**

TABLE OF CONTENTS

1. INTRODUCTION

Any time a remote sensing platform is proposed to be flown in a high radiation environment, scientists and engineers are presented with the challenge of balancing the radiation tolerance of the payload and the spacecraft with mission trajectory and other factors. For a payload with detectors susceptible to noise caused by high fluxes of penetrating radiation (e.g. cameras, spectrometers), the problem becomes a balancing act of shielding, integration time, and time spent in the high flux environment. Various missions in Earth and Jupiter orbit have successfully tackled these issues in the past (e.g. *AMPTE* [1] and *Galileo* [2]) by minimizing the exposure time and maximizing distance to the source and the amount of shielding. *Juno* [3], currently on its way to Jupiter, and the *Radiation Belt Storm Probes* (*RBSP*) [4], to be launched in September 2012 into the heart of Earth's radiation belts, are the latest to prove their radiation mitigation approaches. *Juno* tackles the problem by keeping most of electronics in a 330 mil titanium vault and using an elliptical orbit designed to avoid the most intense portion of the belts [3]. *RBSP* shields all of its electronics boxes separately with 350 mils of Al or higher [4]. An extreme example is the *Jupiter Europa Orbiter* (*JEO*) concept, which would receive a total ionization dose of 2.9 Mrads (behind 100 mils of Al) in orbit around Europa, a moon of Jupiter. This concept envisions a thorough radiation mitigation program, beyond shielding and trajectory mitigation, that involves the natural shielding provided by the moon, maturation of radiation environment and effects models, restriction to approved radiation-hardened parts, improved analysis techniques at both circuit and system levels, and a robust oversight process [5].

This paper presents a mission concept, *Io Volcano Observer (IVO),* to Io, the innermost large moon of Jupiter, and its approach to mitigating the harsh Jovian environment by use of an innovative trajectory, a compact and agile spacecraft, and a payload that is specifically designed for rapid flybys. This concept was selected for and studied via NASA's Discovery and Scout Mission Capabilities Enhancement (DSMCE) program in 2009, specifically for missions enabled by the use of the Advanced Stirling Radioisotope Generators (ASRGs). The results of this study [6] were sufficiently encouraging to proceed, and an *IVO* step-1 proposal was submitted to Discovery 2010. The proposal was ranked "selectable" but was not selected for Phase A study. The overall science objectives of *IVO* were to:

- Understand the eruption and emplacement of Io's currently active lavas and plumes.
- Determine the melt state of Io's mantle and map heat flow patterns to distinguish between shallow and deep-mantle tidal heating.
- Determine the state of Io's lithosphere and understand its tectonic processes via observations of mountains and paterae.
- Understand Io's surface- plume -atmosphere compositions and interactions.
- Understand Io's mass loss, exosphere, and magnetospheric interactions.

From the start of the *IVO* concept study, a systems level approach was adopted to mitigate the risk of flying through the Jovian radiation belts. Section 2 of the paper describes the Io radiation environment. Section 3 explains the trajectory for the flybys, and the total dose and peak fluxes seen by the spacecraft. The time spent in the high intensity environment is also shown. Section 4 addresses mitigation of the high intensity radiation for the payload consisting of Narrow-Angle Camera (NAC), Wide-Angle Camera (WAC), dual Fluxgate Magnetometers (FGM), Thermal Mapper (ThM) and Ion Neutral Mass Spectrometer (INMS)/ Plasma Ion Analyzer (PIA) Package (IPP). We conclude with a description of the overall mission and spacecraft approach, and trades conducted to facilitate a lower total ionization dose.

2. IO RADIATION ENVIRONMENT

In this section, Io's radiation environment is compared with Europa's, since much has been written about the latter and its challenges for spacecraft and instrumentation. It is noteworthy that the Galileo spacecraft and several others (during their flybys) have survived in this environment despite the high dose received by the components. The cold plasma densities are believed to be a factor of 10 higher at Io than at Europa [7]. These low energy particles have a role in spacecraft charging and other issues, however, the primary concern for the sensors and the spacecraft is the penetrating radiation. Europa's orbit (r~9.4 R_J) is close to the peak intensity of the ion radiation belts of Jupiter. Inward of that distance, the measured ion intensities drop off toward Io's orbit. For example, the density (1/cm^3) of ~50 keV to ~50 MeV ions near Io's orbit could be about a factor of 100 times lower than near Europa's orbit [8]. Ion energy spectra data near Io's orbit also exhibited intensities below the Europa's levels [9]. This decrease is likely because ions moving inward from about Europa's distance undergo charge-exchange collisions with the dense neutrals that make up the Io gas torus. Energetic ions that undergo charge-exchange can exit the system as energetic neutral atoms (ENAs), leaving behind a cold ion. This process tends to degrade the ionic radiation belts at the radial distance of Io's neutral gas torus and makes Io's environment somewhat more hospitable than Europa's from the point of view of energetic ions.

In contrast, the energetic electron fluxes are roughly comparable in the environments near Io and Europa at energies between about 100 keV and 1 MeV [9]. Based on *Galileo* Energetic Particle Detector data, electron fluxes in

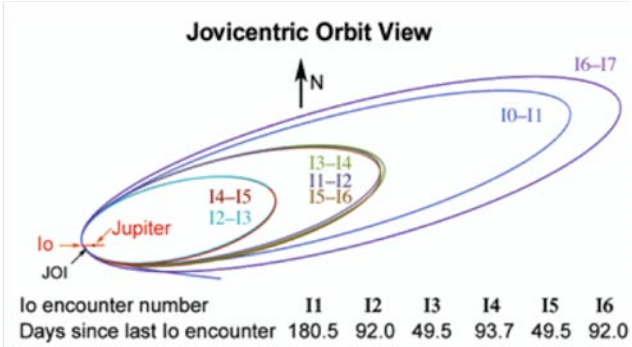

Figure 1 - The Jupiter Orbit Phase Trajectory. The 42°–51° inclination and high-eccentricity orbit offer benefits of low radiation dosage and near polar flyby geometry relative to Io, best for key science objectives.

the 1.5–10 MeV and > 2 MeV and >11 MeV ranges tend to increase inward of Europa's orbit [10]. This trend is consistent with our knowledge of radiation belt structure where the most energetic particles tend to be held more closely to the planet. Also synchrotron measurements near the planet suggest presence of tens of MeV electrons at low Jovian altitude [11].

In summary, it is anticipated that Io will be in a harsher environment than Europa for very energetic electrons. To mitigate this environment, a multipronged approach is adopted, where the radiation design is treated on a mission system level and is a driver for trajectory, payload and spacecraft subsystems as described in the following sections.

3. Trajectory Design

The mission concept begins with a launch from Cape Canaveral Air Force Station onto a heliocentric Venus-Earth-Earth Gravity Assist trajectory. Launch opportunities recur every couple of years on average [5]. One Deep Space Maneuver (DSM) is executed before arrival to the Jovian system six years later. A 51-minute insertion burn settles

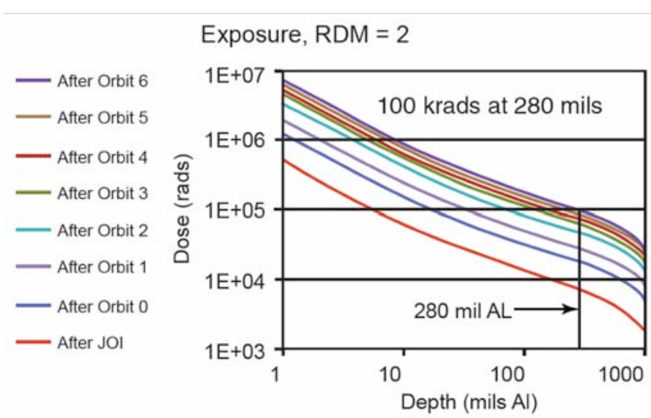

Figure 2 - *IVO* trajectory minimizes the radiation total dose. The design point is set to the total dose after orbit 6 with RDM of 2.

IVO into a 42° inclination, 5.6 Jupiter radii by 180-day orbit. Perijove occurs <1 minute after the end of Jupiter Orbit Insertion (JOI), followed 1.5 hours later by a 10,210-km periapse altitude Io encounter over Io's sub-Jovian hemisphere (designated I0). This relatively distant Io encounter not only reduces JOI ΔV, but also offers unique science and practice for science operations in subsequent Io encounters. During the two- year primary science mission, the S/C accomplishes six more Io encounters (designated I1-I6) with Io near perijove by using successive orbits in resonance with Io's orbit, as shown in Figure 1.

Small statistical Trajectory Correction Maneuvers (TCM) ~12 and ~3 days before each Io encounter refine targeting of the encounter, and a statistical TCM 3–5 days after corrects encounter targeting before each apojove TCM. Trajectory propagation accounts for perturbations using higher-order gravity models for Jupiter and Io, and point-mass gravitational center of attraction for icy Galilean moons.

IVO's orbit is optimized for Io science objectives by providing unique polar observations to test tidal heating models, similar illumination for repeat observations to map rapid surface changes, and ideal geometry for magnetospheric sounding.

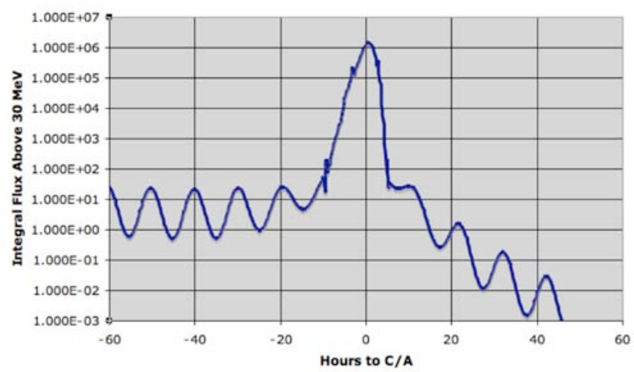

Figure 3 - Integral flux above 30 MeV (assuming ~1 cm Ta shielding) versus time to closest approach in a typical Io encounter.

To reduce the orbit period from 180 days to near the minimum allowable 49.5 days, a duration based on time needed to transmit acquired data, Io encounters I1 and I2 are nightside passes near Io's leading hemisphere. During these encounters, hot spot and limb plume searches are conducted. Two of the encounters (I3 & I5) are optimized for measurement of the induced magnetic signature from mantle melt [12], via nearly identical flyby geometries, one near the maximum magnetic latitude and the other near its minimum. These geometries are achieved using dayside low-phase flybys near the Pele plume and directly over the 18 km high Boosaule Montes. They also avoid Io's wake (leading its orbital motion) to minimize plasma effects. I4 uses a leading side nightside periapsis to lower the orbit period in advance of I5. I4 is a 178-km altitude flyby optimized for surface composition measurements by INMS and hot spot observations. I6 achieves a 179-km altitude flyby over the giant Loki Patera,

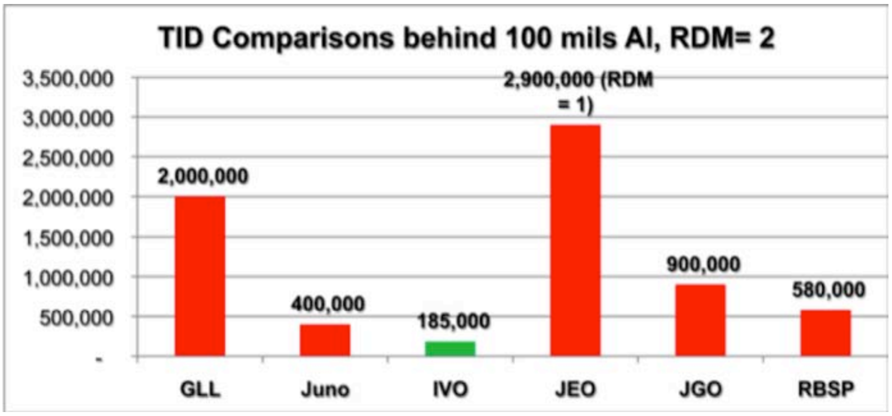

Figure 4 - Total Ionizing Dose (TID) for past and potential future Jupiter missions, normalized to 100 mils Al shielding and with a radiation design margin of 2 except for *JEO* (RDM = 1) and *Galileo* (actual estimated TID for full mission). Also shown is the expected TID for the *Radiation Belt Storm Probes* mission.

leading to a return to the vicinity of Io 207 days later for a potential extended mission. The spacecraft nominally collects and records 20 Gb of science data per encounter - 100 times the Io data return from the *Galileo* mission over 8 years. The data is relayed to Earth near apoapsis.

IVO's orbit is also optimized to minimize total ionizing dose (TID). The orbit is inclined ~42–51º to Jupiter's orbital plane, leading to more north-south flybys near Io. This geometry minimizes total dose per flyby because the spacecraft passes through the high-radiation zone at high velocity (16–19 km/s range) and the glancing angle reduces time in the most intense parts of the belts, near the equator. The radiation environment was modeled using the Galileo

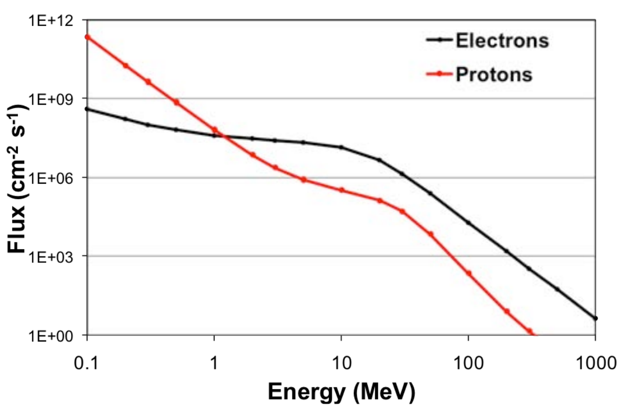

Figure 5 - Peak integral flux for electrons and protons. The 1 cm Ta shielding of the NAC/ WAC detectors eliminates the radiation noise from protons below 100 MeV and electrons below 30 MeV.

Interim Electron Model (GIRE) [13, 14, 15]. The model was used to predict the proton and electron fluence for mission trajectories in the Jovian orbit. The GIRE outputs were fed into the ShieldDose-2 [16] code to produce the dose depth data for each orbit, as shown in Figure 2. The resultant dose is just ~10 krad TID per flyby (behind 100 mils Al), versus ~85 krad/flyby for the *JEO* as studied in October 2008. The spacecraft spends only ~15 hrs/flyby in the intense radiation (see Figure 3). The TID of *IVO* is significantly less than that of other Jupiter orbiters, as demonstrated in Figure 4.

The pole-to-pole flyby geometry is best for probing Io's interior with the magnetometers, and the spacecraft gets closer to Io with low radiation-induced noise for measuring faint emissions when Io is in eclipse. Furthermore, the approach and departure geometry provides excellent views of the polar regions, key to testing tidal heating models and atmospheric models. The subsolar longitude changes slowly with each encounter, since the Jupiter year is 12 years long; this repeat coverage is best for change detection to understand active processes and resurfacing rates. Large margins in propellant and radiation hardness offer the potential for a significant extended mission. Following an extended mission, the spacecraft would impact into Io or Jupiter.

4. Payload Design

The payload is designed to operate during the fast flybys and peak radiation fluxes, which are shown in Figure 5. The impact of radiation-induced transient noise on the payload detectors was analyzed by estimating the number of high-energy electrons and protons penetrating the radiation shield, and evaluating their effect on the detector material, following the *JEO* approach [17]. During Io flybys, the total integrated flux of incident electrons was estimated to be 3.5 $\times 10^6$ electrons/ (cm^2·s) for 1 cm Ta shielding. The flux of incident protons reaching the detector was estimated by applying a 100-MeV cutoff energy to the external integral proton flux. For 1 cm of Ta shielding (e.g. for NAC / WAC detectors), about 920 protons/cm^2·s reach the detectors during Io flybys. The radiation shielding analysis and the signal to noise (SNR) calculations presented in the following sections are based on the prevalence of electrons in the Ionian environment. The mass allocated for instrument shielding is shown in Table 1. The instrument detector shielding is carried as a separate line item since the detectors are specifically shielded against the peak flux, versus TID for the electronics boxes.

TABLE 1
PAYLOAD SHIELDING MASS ALLOCATIONS

Component	Shielding Mass Allocation (kg)
Narrow-Angle Camera (NAC) Detector	0.9
Wide-Angle Camera (WAC) Detector	0.9
NAC/ WAC Data Processing Unit (DPU)	1.8
Ion and Neutral Mass Spectrometer (INMS) Detectors	2.0
Plasma Ion Analyzer (PIA) Detectors	2.9
INMS/PIA DPU	2.5
Fluxgate Magnetometer DPU	1.8
Thermal Mapper Front End Electronics	2.0
ThM DPU	1.8
Total CBE Mass (kg)	16.6
Contingency	30%
Total Mass (kg)	21.6

Narrow- Angle Camera (NAC) and Wide-Angle Camera (WAC) Designs

The NAC is key to many *IVO* objectives. The NAC envisioned here would have a 5 µrad/pixel instantaneous field of view (IFOV), like LORRI on *New Horizon*s [18], but with a new 2K x 2K detector and more capable data processing unit (DPU). Half of the array is covered by 14 color bandpasses in 64-line stripes, and half of the array is clear for framing images and movies. The color images are acquired in pushbroom mode, adding up to 64 rows for digital time-delay integration (dTDI). The NAC characteristics are shown in Table 2.

The detector uses Complementary Metal Oxide Semiconductor (CMOS) technology for scientific performance [19] that features low read noise, good modulation transfer function (MTF), large dynamic range, and a large spectral range. For *IVO*, the advantages of CMOS over charge-coupled device (CCD) technology are (1) very fast readout times, (2) imaging in either pushbroom or framing modes, (3) low power, and (4) less degradation in performance after a high total ionizing dose (TID). The tolerance to TID (no measurable degradation after 100 krad from energetic electrons) far exceeds *IVO*'s requirement (<10 krad) inside 1-cm Ta shielding. On-chip correlated double sampling eliminates row-settling time for fast readout (0.025 µs/pixel, >500x faster than *Galileo* Solid State Imaging), minimizing radiation-induced noise (see Table 3).

The NAC DPU is derived from previous JHU/APL DPUs, such as *MRO* CRISM [20] and LORRI support electronics, and with more capable FPGAs for implementation of dTDI and memory-efficient wavelet compression algorithms [21].

The WAC will have a field of view of ~26° (200 µrad/pixel) to enable along track stereo mapping, key to several science objectives, as well as to cover a larger area on Io than the NAC when at close range. It will utilize an identical focal plane system (FPS) and DPU as the NAC, and will also have 14 color bandpasses and a framing area. The WAC optics are a foreign contribution, designed by FISBA Optik AG, using a variety of radiation hard glasses with radiation tolerance up to 10 Mrad with 2% degradation within the WAC wavelength range.

TABLE 2
NAC AND WAC INSTRUMENT CHARACTERISTICS

Parameter	NAC	WAC
Wavelength range	200-1100 nm	400-1100 nm
FOV	0.58° x 0.58°	26° x 26°
IFOV	4.95 µr/pixel	217 µr/pixel
Scale @ 1000 km	4.95 m/pixel	217 m/pixel
Aperture	150 mm	12.25 mm
f/#	16.7	3.0
Optical efficiency	>63%	>80% @ 600 nm
System MTF	>0.2 at Nyquist	>0.2 at Nyquist
Size	51x15.3x15.3 cm	33x15.3x15.3 cm
Mass (w/o shielding)	8.3 kg	4.8 kg

TABLE 3
NAC/WAC FOCAL PLANE SYSTEM AND ELECTRONICS

Characteristic	Value
CMOS Array	2048 x 2048 pixels
Pixel size	10-µm
Pixel type	5T PPD
Quantization	14 bits
Quantum efficiency(QE)	0.3 @ 600 nm
Inverse gains	2 e^-/DN (high gain) or 8e^-/DN (low gain)
Read noise	2.5 e^- (high gain) or 10 e^-
Full well	30k e^- (high gain) or 120K e^-
Color filters	14
Compression	Look-Up Tables, wavelets
Exposure control	Automatic or manual
Operational power	4.8 W
Decontam. Power	12 W
Bandwidth FPS to DPU	560 Mb/s via 4 ports
Bandwidth to Solid State Recorder	25 Mb/s

TABLE 4
SELECTED NAC IMAGES OF IO AND SNR CALCULATIONS

Range to Io (km)	Pixel binning	Swath width (pixels)	# dTDI lines	# colors	Color bandpass transmission	Typical daytime SNR	SNR for 1473 K lava
200	2	500	9	1	1.0 (clear)	34	239
1000	1	1000	11	1	1.0 (clear)	42	295
5000	1	2048	30	4	0.2	78	894
60000	1	2048	48	8	0.1	125	N/A[1]
200000	1	2048	32	12	0.1	230	N/A[1]

[1]Hot lava fills very small fraction of pixel larger than ~100 m

TABLE 5
SELECTED WAC IMAGES OF IO AND SNR CALCULATIONS

Range to Io (km)	Pixel binning	Swath width (pixels)	# dTDI lines	# colors	Color bandpass transmission	Typical daytime SNR	SNR for 1473 K lava
200	1	2048	1	10	1.0 (clear)	275	saturated
200	1	2048	1	10	0.2 (color)	109	766
1000	1	2048	4	10	1.0	436	N/A
1000	1	2048	4	10	0.1	130	N/A
200	1	2048	1	10	1.0 (clear)	275	saturated

Detailed SNR calculations for NAC and WAC have been completed that include the exact exposure and readout times and expected energetic particle flux and induced RMS noise behind 1 cm Ta [17, 22], as well as read noise (2.5 or 10 e^-) and shot noise (square root of signal in e^-). The more challenging results apply to the NAC; WAC SNRs are typically ~10x larger than for the NAC under identical conditions because the WAC accepts more signal per pixel per sec and can utilize much longer exposure times during the fast flybys. An equivalent of 1 cm Ta shielding around the WAC FPS, identical to the NAC is assumed; some of this shielding is provided by the glass optical elements rather than by metal. There are two stressing cases (for the NAC): (1) near closest approach at a relative velocity of 16–19 km/s (described above), and (2) imaging faint emissions through the mid-ultraviolet and narrow bandpasses when relatively far from Io as signal levels are quite low making SNR low (<50:1) in spite of negligible radiation-induced noise. The faint emissions cannot be usefully imaged when *IVO* is inside the radiation belt.

For the closest approach imaging, the NAC has very short line times (e.g., 0.28 ms @1000 km), but can achieve 40:1 SNR for clear-filter pushbroom imaging with a 1000-pixel swath and 11 dTDI lines (Table 4). Higher SNRs are possible by binning or by sacrificing swath width to allow more dTDI lines. The 40 Mpixel/s transfer rate to the DPU forces a tradeoff between swath width, number of TDI lines, and number of color images when near Io. Note that SNRs over Io's hot lavas (daytime or nighttime imaging) can be much higher if a significant fraction of the pixel is filled by liquid lava temperatures. With the WAC, 7 color and 3 clear (stereo) pushbroom images are acquired with >100:1 SNR during an 18 km/s flyby at ~ 200 km or larger ranges (Table 5). Moreover, the WAC can even image the night side of Io's Jupiter-facing hemisphere, illuminated by Jupitershine, with SNR 16:1 at 200 m/pixel scale.

These SNR calculations assume a frontside-illuminated CMOS detector with a peak quantum efficiency (QE) of just 0.3. However, backside thinning and illumination are being considered, which roughly doubles the clear-bandpass QE, and more than doubles the ultraviolet QE, and thus would significantly improve SNRs.

Dual Fluxgate Magnetometers (FGM)

The FGM achieves the second objective listed in Section 1 by mapping the magnetic field strength and variability to distinguish between melt states of Io's mantle. To meet these requirements, the FGM design includes 0.5% absolute accuracy (0.25 nT at 50 nT), and 0.12-nT sensitivity. To meet the S/C settling time requirement (for imaging), a long flexible boom is excluded and dual FGM sensors (for identification and removal of S/C variable fields) are needed. The sensors are mounted on the high gain antenna (HGA) and on the top of the spacecraft deck, following the same approach used for *Near Earth Asteroid Rendezvous* and *Venus Express* missions. Both FGM sensors operate continuously at Jupiter at a low sampling rate (1 vector/s). Within 20 Io radii the rate increases to 30 vectors/s. The DPU is based on the *MESSENGER* design with use of standard 100 krad parts, and is shielded with equivalent 280 mils of Aluminum. The instrument weighs 2.9 kg, and uses 3.3 W of operational power.

Thermal Mapper (ThM) Design

The ThM design is very similar to the Thermal Emission Imaging System (THEMIS) on *Mars Odyssey* [23], but with

TABLE 6
THERMAL MAPPER INSTRUMENT CHARACTERISTICS

Characteristic	Value
Wavelength Range	1.5-30 µm
FOV	4.6° cross track, 3.5° along track
IFOV	125 µrad/pixel
Aperture	12 cm
f/#	1.6
Detector size	640 x 480 pixels
Pixel Size	25 µm
Filters	10
Sensor mass (w/o shielding)	8.8 kg
Operational Power	9.3 W

an improved microbolometer detector, increased radiation shielding or radiation-hardened part selections, and excludes the visible imager. ThM characteristics are summarized in Table 6. Also, for *IVO* the spectral bandpasses extend from 2-5 microns (to study cooling lavas) to 30 microns (to measure the background temperatures). There are also several bandpasses in the 7–12 micron region for silicate mineralogy. Only the still-warm lavas provide sufficient signal to measure the small emission variations with wavelength, and these are also the only regions free of SO_2 frost cover. A spatial resolution of tens of km is adequate to measure the global heat flow, but km-scale resolution is best for silicate mineralogy. High SNR is achieved in appropriate bandpasses for expected range of temperatures that the ThM will map (~80-1200 K). At 240 K, the NEΔT achieved is 0.2 K; at 1000 K, it is ~ 5 K. Low temperatures are the most challenging, but NEΔT < 2 K at 80 K is achieved in 10- to 30- micron bands.

The microbolometer detector technology is ideal for the radiation environment near Io, because energetic particles pass through the thin films with little interaction [17]. Hence, radiation-induced noise is not a problem, in contrast to the severe challenge of near-infrared reflectance spectroscopy. The detector readout circuit was tested to only 20 krad for THEMIS. However, in its spacecraft location, it is protected by the DPU (with >280 mils of Al) and by the spacecraft panels. Additional mass was allocated for the spot shielding to be designed in Phase A (Table 2), if further radiation modeling shows the need for additional shielding.

TABLE 7
INMS INSTRUMENT CHARACTERISTICS

Characteristic	Value
Mass range	1 – 300 amu (low mass range) 1 – 1000 amu (high mass range)
Mass resolution (M/ΔM)	1100
Sensitivity, for 5 – s integration	10^{-15} mbar
TOF channels, horiz.	65536
TOF resolution	0.5 ns
TOF channels, vert.	24 bit
Dynamic range, per spectrum	> 7 decades
Sensor mass (per 1 INMS, w/o shielding)	1.5 kg
Operational Power (per INMS)	4.5 W

Ion and Neutral Mass Spectrometer/ Plasma Ion Analyzer Package (IPP)

The IPP consists of dual Ion and Neutral Mass Spectrometers (INMS) and dual Plasma Ion Analyzers (PIA), with shared electronics. One INMS is located on the ram-facing side of the spacecraft; the second INMS is on the opposite side of the spacecraft. The two PIA instruments are placed such that the combined field-of-view covers 4π ster.

INMS science objectives include measuring abundances of neutral and ionized species in atmosphere, plumes, exosphere and plasma torus, and measuring plume species (S, O, SO_2, S_2, SO, Na, K, Cl, and unknown species) to model equilibrium chemistry of magma chambers. INMS has a high potential for new discoveries because the composition and abundances of neutrals escaping from Io are poorly known.

INMS is a time-of-flight instrument (TOF) [24], which allows for recording a full mass spectrum at once. Typically, 10,000 mass spectra are recorded each second, and accumulated for 5 seconds. Thus, the accumulated spectrum features a dynamic range of 10^7. The accumulation time can be adjusted by command to optimize for the observation conditions during the flybys. Table 7 summarizes the key parameters of the INMS instrument.

Penetrating radiation limits the dynamic range of the INMS measurement significantly because of elevated background count rates in the Microchannel Plate (MCP) detector, which is located at the periphery of the instrument. Without radiation shielding of the detector the flux of $3 \cdot 10^8$ $e^-/(cm^2$ s) will cause approximately 500 background counts in each 0.5-ns bin of the TOF spectrum accumulated for 5 seconds.

TABLE 8
PIA INSTRUMENT CHARACTERISTICS

Characteristic	Value
Mass range	1-70 amu
Mass resolution (M/ΔM)	5-8
Viewing angle	360^o x 90^o (2π)
Angular resolution	22.5^o x 12^o
IFOV	360^o x 12^o (16 sectors)
Energy Range	10 eV- 15 keV
ΔE/E	0.07
Sensor mass (per 1 PIA, w/o shielding)	0.9 kg
Operational Power	2.5W

This limits the dynamic range to about 4 decades and reduces the life-time of the MCPs because of the high extracted charge. To reduce the flux of penetrating radiation on the MCPs, a multi-layer radiation shield has been designed using Al and Ta that reduces the penetrating electron flux to $4 \cdot 10^4$ $e^-/(cm^2\ s)$, although results in secondary γ-radiation of $5 \cdot 10^5$ $\gamma/(cm^2\ s)$. But even with the high secondary flux, this radiation shielding strategy improves the dynamic range to 6 decades and allows measurement of trace species in Io's atmosphere even at the closest approach.

PIA science objectives include measurement of the density, energy, and temporal variability of plasma near Io, both to better understand plasma interactions and to calibrate plasma contributions to the magnetic signature of mantle melt.

PIA is an extremely lightweight TOF sensor based on successful Solar Wind Monitor instrument on *Chandrayaan-1* [25] and Detector for Ions on Mars built for *Phobos-Grunt*. Table 8 summarizes its key characteristics. All of its heritage electronics were developed for a > 100 krad environment, and additional shielding has been allocated to mitigate the higher radiation environment of Io. The spot shielding is being developed as part of preparation for the Jupiter Europa Icy Moons proposal in early 2012.

The shared electronics for IPP integrates the INMS and the PIA electronics, including the data processing, HVPS, and DC/DC converters and provides spacecraft interfaces. It weighs 4.3 kg, and uses 5.8 W of power and is shielded by 280 mils of Aluminum.

5. Mission and Spacecraft Design

Mission Trades

As part of this study, a trade on the radiation mitigation approach was conducted. The vault (*Juno* approach) and unit shielding (*RBSP* approach) were considered. The trade resulted in the use of unit shielding, since the total shielding mass (for spacecraft and payload) was found to be lower when individual boxes were shielded by 280 mils to 100 krad with RDM of 2. The breakdown of the shielding mass by box is shown in Table 9. Radiation-hard parts rated at 100 krads are used in all electronics, where possible, without compromising heritage. Components that were heritage based and did not have 100 krad parts were additionally spot shielded to 100 krad levels.

The star tracker utilizes a similar approach to *Juno* and *JEO*, with SELEX Galileo Avionica supplying the *Juno* modified A-STR. The star tracker head and electronics unit are split, and the additional shielding is added to the electronics unit to get to 100 krads with RDM of 2. To shield against peak flux, the *Juno* star trackers use an equivalent 3.4 inches of aluminum shielding in the optical head, protecting the CCD. The peak integral flux for *IVO* is 5 times less than that for *Juno*, so additional shielding was not needed to mitigate the environment. However, during the peak flux time period at the closest approach, the star tracker is expected to have difficulty distinguishing between Single Event Upsets (SEU) and real stars. In *Juno*'s case, outages of up to 30 minutes are expected as *Juno* crosses the radiation belts. During the design phase the *IVO* project will perform detailed analyses with the star tracker vendor to determine the SEU performance in the specific environments to be experienced, although some outage time is expected to occur during the science encounters. During these periods the attitude control will use an onboard solution that propagates the last valid tracker ephemeris with IMU data. To help maintain the required accuracy, an extended Kalman filter will compensate for observed, measured IMU drift and bias; IMU performance will be measured throughout *IVO*'s cruise and science phases to build up a substantial performance baseline, while the unit temperatures in the outer solar system are stable enough to minimize thermal variations.

TABLE 9
Spacecraft Component Shielding Mass Breakdown

Component	Shielding Mass Allocation (kg)
Traveling Wave Tube Amplifier	2.6
Electrical Power Conditioner	3.0
Star Tracker	0.0*
Power System Electronics	0.0*
Battery	0.0*
Power Distribution Unit	5.2
Integrated Electronics Module	7.9
Inertial Measurement Unit	5.9
Propulsion Diode Box	4.0
Transceiver	3.2
ASRG Controller Units	10.9
Sun Sensors	1.9
Sun Sensor Electronics	2.9
Total CBE Mass (kg)	47.5
Contingency	30%
Total Mass (kg)	61.8

* see text for further discussion

Radiation engineering was applied to all of the spacecraft electronics. Several components, e.g. power system electronics and battery were *RBSP* heritage designs with 350 mils of Al equivalent chassis. These components remained unchanged. A 32-Gb solid state recorder accommodated the desired flyby science data volume of 20 Gb, and also supported lapses in communication due to conjunctions or in the event of missed downlink opportunities. Modern flash memory capabilities permit its use in higher radiation environments, such as the Samsung 4Gb NAND single-level flash whose baseline is radiation-

TABLE 10
MISSION FUNCTIONAL REQUIREMENTS

Mission Requirements
S/C settling time for NAC is ≤ 100 s after S/C turns of 90°
S/C slews (rotate) from 0.05 to 8 mrads/s
Scan rate knowledge (to NAC) of 3.1 µrad/s reported ~ 5 s after thruster firing
Pointing stability up to 36 µrad/s
Pointing accuracy to 1 mrad (10% of NAC FOV)
Simultaneous data collection from NAC/WAC, FGM, ThM, and INMS/PIA during the closest approach

hard to at least 100 krad prior to the additional shielding applied to the integrated electronics module that it is contained within. The ASRGs and their Controller Units (ACUs) are designed for natural radiation environment of 50 krads behind 60-mil aluminum shield [26], in addition to exposure to its self-generated ionizing radiation. All ACU EEE parts were rated at 100 krad. In this concept, the ACUs were shielded additionally to the total of 280 mils of Al equivalent. This radiation design philosophy was very conservative: not only the RDM of 2 applied for all of the individual boxes, but the calculations did not include the protection individual boxes gain from placement neighboring each other. Significant mass margins carried at the spacecraft level (55% margin over the current best estimate dry mass) allowed additional flexibility for Phase A trades on shielding optimization. More complex ray-trace analysis in FASTRAD and radiation transport physics analysis in Novice as the spacecraft design matures would provide the detailed TID distributions and allow spot shielding of critical devices that do not meet the 100-krad requirement.

Spacecraft Design

The spacecraft has been designed to accommodate fast flybys of Io, while protecting the sensitive components from radiation. The driving mission requirements are listed in Table 10. The spacecraft accommodates these requirements by use of three-axis control with twelve 0.9 N coupled thrusters aligned with spacecraft mechanical axes and four 4.4 N attitude control system thrusters used for slews about Y-axis. The settling time was minimized by explicit avoidance of flexible appendages: the spacecraft was powered by two ASRGs (instead of the solar panels which would significantly degrade maneuverability), and the FGM sensors were mounted directly on the spacecraft body. Redundant star trackers and inertial measurement units reused the *New Horizons* G&C algorithms. Because of the rapid flybys and use of the ASRGs, the spacecraft could take advantage of a store-and-forward architecture, where the data are collected rapidly during the flyby, stored on a solid state recorder that supported the concurrent data flow from all payload elements, and played back to Earth during the 40+ days after each flyby. The use of ASRGs also constrained the total amount of power available to the spacecraft. During maneuvers (s.a. JOI, DSM and TCMs), a 50 A-hr battery was used.

6. CONCLUSION

The *IVO* concept is the first dedicated in-depth study of the most volcanically active world in the Solar System, Jupiter's moon Io. It draws upon the radiation mitigation approaches of other missions such as *Juno* and *RBSP*, and on experience with effects of radiation on payload from *Galileo*. The systems approach to radiation engineering from the spacecraft-level to the part-level results in a robust design, where radiation tolerance is derived from a combination of an inclined trajectory, shielding of sensitive electronics and selection of radiation-hard parts.

REFERENCES

[1] B. Hausler et al., "The AMPTE IRM Spacecraft," *IEEE Trans. on Geoscience and Remote Sensing*, vol. GE-23, no. 3, pp 192-201, May 1985.

[2] P.D. Fieseler, S.M. Ardalan, and A.R. Frederickson, "The Radiation effects on Galileo spacecraft systems at Jupiter", *IEEE Trans. Nucl. Sci.*, vol. 49, pp 2739-2758, 2002.

[3] R.S. Grammier, "A look inside the Juno Mission to Jupiter", in *Proc. Aerospace Conf.*, Big Sky Montana, pg. 1-10, 2009.

[4] K. Kirby et al., "Radiation Belt Storm Probe Spacecraft and Impact of Environment on Spacecraft Design", in preparation for this conference, 2011.

[5] K. Clark et al., JEO study, http://opfm.jpl.nasa.gov/, 2008.

[6] A. McEwen, A. et al., "Io Volcanic Observer (IVO)",in *Proc. Lunar Planet. Sci. Conf. 40,* 1876, 2009.

[7] M. G. Kivelson et al., "Magnetospheric Interactions with satellites," in *Jupiter: The Planet, Satellites and Magnetosphere*, F. Bagenal, T.Dowling and W. McKinnon (Eds.), pp.513-536, Cambridge University Press, Cambridge, 2004.

[8] B. H. Mauk et al., "Energetic ion characteristics and neutral gas interactions in Jupiter's magnetosphere", *J. Geophys. Res.*, vol. 109, A09S12, doi:10.1029/2003JA010270, 2004.

[9] C. Paranicas et al., "The radiation environment near Io", *Geophys. Res. Letters*, vol. 30, pp. 1919, 2003.

[10] I. Jun et al., "Statistics of the variations of the high-energy electron population between 7 and 28 jovian radii as measured by the Galileo spacecraft", *Icarus*, 178, pp.386-394, 2005.

[11] S.J. Bolton et al., "Ultra-relativistic electrons in Jupiter's radiation belts", *Nature*, vol. 415, pp.-987-991, 2002.

[12] K. Khurana et al.," Evidence of a global magma ocean in Io's interior", *Science*, vol. 332, p. 1186, 2011.

[13] N. Divine, "Charged particle distributions in Jupiter's magnetosphere", *J. Geophys. Res.*, vol. 88, pp. 6889-6903, 1983.

[14] H.B. Garret, "Galileo Interim Radiation Electron Model", JPL Publication 03-006, 2003.

[15] I. Jun, "High-energy trapped particle environment at Jupiter: An update", *IEEE Trans. Nucl. Sci.*, vol. 50, pp. 2281-2286, 2003.

[16] M. Seltzer, "Updated calculations for routine space-shielding radiation dose estimates: SHIELDOSE-2", *NIST Publication NISTIR 5477*, Gaithersburg, MD, 1994.

[17] J. Boldt et al., "Assessment of radiation effects on science and engineering detectors for the JEO Mission study", JPL D-48256, 2008.

[18] A. Cheng et al., "Long-Range Reconnaissance Imager on New Horizons. *Space Sci Rev.,* vol. 140, pp. 189–215, 2007.

[19] J. Janesick et al., "Fundamental performance differences of CMOS and CCD imagers: Part IV", *Proc. SPIE* 7742-11, San Diego, 2010.

[20] S. Murchie et al., "Compact Reconnaissance Imaging Spectrometer for Mars (CRISM) on Mars Reconnaissance Orbiter (MRO)", *J. Geophys. Res.,* vol. 112*,* E05S03, doi:10.1029/ 2006JE002682, 2007.

[21] J.R. Hayes, K. Strohbehn, and G. A Murphy, "Low-cost wavelet image compression for FPGAs", *Proc. SPIE* 7455, 7455D, 2009.

[22] K. Klaasen et al., "Charge-coupled device television camera for NASA's Galileo mission to Jupiter," *Opt. Eng.* , vol. 23, pp. 334-342, 1984.

[23]]P.R. Christensen et al., "The Thermal Emission Imaging System (THEMIS) for the Mars 2001 Odyssey mission", *Space Sci. Rev.,* vol. 110*,* pp. 85–130, 2004.

[24] D. Abplanalp et al.,"A neutral gas mass spectrometer to measure the chemical composition of the stratosphere," *Adv. Space Res*., vol. 44, 870-878, 2009.

[25] S. Barabash et al.,"Investigation of the solar win-Moon interaction onboard Chandrayaan-1 mission with the SARA experiment", Curr. Sci., vol. 96, pp.526-532, 2009.

[26] ASRG User ICD A, 912IC002085, Lockheed Martin Energy Systems, June 2011.

BIOGRAPHIES

Dr. Elena Adams is a systems engineer in the Space Department at the Johns Hopkins Applied Physics Laboratory. She received a B.S. from the University of Virginia, Charlottesville, in Applied Mathematics, a M.E. in Space Systems Engineering from University of Michigan, Ann Arbor, and a M.S. and a Ph.D. in Atmospheric, Oceanic and Space Sciences from the University of Michigan, Ann Arbor. She has worked with a variety of instruments, including Cassini-Huygens GCMS, Juno MWR, and ExoMars MOMA. She is currently supporting RBSP, and a variety of proposals and studies, including Europa Mission study.

Dr. Alfred McEwen is a planetary geologist and professor at the University of Arizona, USA. He has participated in ten deep space missions, including Galileo to Jupiter, for which he led the image observation planning for Io. Currently he is the Principal Investigator of the High Resolution Imaging Science Experiment (HiRISE) on Mars Reconnaissance Orbiter and of the High-resolution Stereo Color Imager (HiSCI) on the 2016 ExoMars Trace Gas Orbiter. In 2011 he received NASA's Distinguished Public Service Medal. For more, see http://www.lpl.arizona.edu/Support/faculty/faculty.php?nom=McEwen.

Kenneth Hibbard received his B.S. in Aerospace Engineering from the Pennsylvania State University, and his M.S. in Systems Engineering from the Johns Hopkins University. He spent eight years as a spacecraft systems and operations engineer at NASA Goddard working on the ACE, SOHO, and Swift spacecraft. At APL, Mr. Hibbard served as the MESSENGER Deputy Mission Operations Manager, and is currently a senior systems engineer supporting multiple programs, proposals, and mission studies. Mr. Hibbard serves as the Formulation Deputy Project Systems Engineer for the Europa mission study, and as the Mission Systems Engineer for the Titan Mare Explorer (TiME) Discovery proposal.

Dr. Elizabeth Turtle is a research scientist in the Planetary Exploration group at APL. She received her B.S. in Physics from MIT and her Ph.D. in Planetary Sciences from the University of Arizona. She was an associate of Galileo's imaging team and is an associate of Cassini's Imaging and RADAR teams and a member of Lunar Reconnaissance Orbiter's Camera team. Her research interests include combining remote sensing observations with modeling to study geological structures, including impact craters on terrestrial planets and icy satellites, mountain formation on Io, and lakes on Titan, as well as seasonal changes in Titan's weather patterns.

Edward Reynolds is Deputy project manager for Solar Probe Plus, and the former project manager for the STEREO mission. Mr. Reynolds received a B.S. in electrical engineering from Virginia Tech. He has an extensive background in spacecraft system engineering, which stems from his experience in spacecraft integration and test. Prior to the STEREO mission, Mr. Reynolds played key engineering roles in several projects, including the Comet Nucleus Tour (CONTOUR) and the Near Earth Asteroid Rendezvous (NEAR), the first mission in NASA's Discovery Program, that orbited and eventually landed on the asteroid Eros. Additionally, he has worked on a number of assignments involving satellites, and sounding rockets with engineers from Russia.

Dr. Nicolas Thomas is a professor of Experimental Physics at the Unviersity of Bern. He received the M.S. in Experimental Space Physics from University of Leicester and his Ph.D in Physics from University of York. He is currently the Co-PI and Hardware Lead for the BepiColombo Laser Altimeter. Previously he has been a lead investigator on Microscope on Beagle 2 lander on Mars Express, a Co-I on the OSIRIS imaging system and the RSI radio science experiment on Rosetta, a Co-I on the HiRISE imaging experiment on Mars Reconnaissance Orbiter amd on DISR imager and spectral radiometer on Cassini/Huygens. He is a past chair of the European Space Agency's Solar System Working Group.

Dr. Philip Christensen is a planetary geologoist and professor at the Arizona State University. He has received the B.S. in Geology and a Ph.D. in Geophysics and Space Physics from University of California Los Angeles. He has been the principal investigator for Mars Odyssey Thermal Emission Imaging System, Mars Rovers Missions Miniature Thermal Emission Spectrometer, Mars Global Surveyor Thermal Emission Spectrometer and a co-investigator on EOS ASTER Mission. He has numerous NASA and Geological Society of America achievement awards, and is a chair for the NRC Decadal Survey Mars Panel.

Dr. Peter Wurz is a professor in Space Research and Planetary Sciences Physics at the University of Bern. He has received his M.S, Ph.D. in Technical Physics from Technical University of Vienna, and Viena Docendi from University of Bern. He is a Principal Investigator for the P-BACE instrument on the MEAP mission, co-Principal Investigator for the LASMA instrument on Phobos-Grunt, and lead Investigator for RTOF instrument of ROSINA on the Rosetta mission. He has been a Co-Investigator on SOHO CELIAS, IMAGE LENA, Mars Express ASPERA-3, Venus Express ASPERA-4, STEREO PLASTIC, BepiColombo SERENA & MPPE/ENA, IBEX IBEX-Lo and Chandrayaan-1 SARA. He has numerous ESA and NASA achievement awards, and is a member of LAPLACE & Bepi-Columbo science definition teams.

Dr. Martin Wieser is a research scientist at the Swedish Institute of Space Physics. He received a Ph.D. in Physics from the University of Bern. He is a Principal Investigator for Phobos-Grunt DIM and PRISMA PRIMA, co-I on MEAP balloon experiment, Chandrayaan-1SARA, Bepi-Colombo MPPE/ENA, SERENA/MIPA and a collaborating scientist for NASA's IBEX mission.

Dr. Christopher Paranicas is a research scientist in the Space Physics group at the Johns Hopkins University Applied Physics Laboratory. He received his B.A. in Physics from Harward College, and his Ph.D. in Physics from Columbia University. He is a Co-Investigator, Magnetospheric Imaging Instrument (MIMI) on the Cassini orbiter, member of the Joint Jupiter Science Definition Team (EJSM mission) and has been a participating scientist on Galileo EPD, New Horizons PEPSSI, Juno JEDI, Voyagers 1 and 2 LECP instruments.

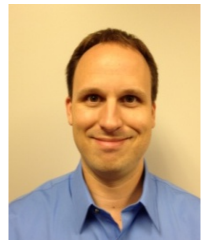

Gabe Rogers is a section supervisor in the Mission Design, Guidance, and Control Group in the APL's Space Department. He received a B.S. in 1995 and M.S. in 1997 from the University of Illinois in Aeronautical and Astronautical Engineering. He joined APL in 1997, and has worked on several NASA sponsored missions, including NEAR, CONTOUR, TIMED, MESSENGER, and STEREO. He is currently the G&C lead for the New Horizons and RBSP missions, and a technical contract representative for the Solar Probe Plus mission.

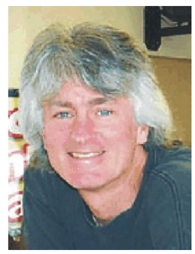

Jim Janesick is currently a Director of the Advanced Sensors Group at the SRI Sarnoff. He holds a B.S. in electronics and electrical engineering from California Polytechnic University, and an M.S. in electronics engineering from University of California, Irvine. At Sarnoff Inc., he develops high-performance CMOS sensors for scientific and government imaging. Previously, at Conexant Systems Inc., he has developed commercial CMOS imagers. At Pixel Vision, Inc., Mr. Janesick developed high-speed backside illuminated CCDs for scientific and cinema photography applications. At JPL, he pioneered scientific CCD and support electronic designs for several NASA space-based imaging systems, including the Hubble Space Telescope, Galileo, Cassini, Multi-Imaging Spectral Radiometer, Solar X-ray Telescope, Mars Orbital Camera, Mars Pathfinder, DS I, New Horizons, and Stardust. He holds numerous NASA medals for Exceptional Engineering, and is a SPIE fellow.

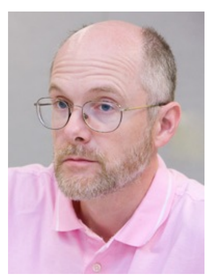

Dr. Brian J. Anderson is Principal Staff Physicist with The Johns Hopkins University Applied Physics Laboratory with extensive experience in space magnetometry and spacecraft magnetic field mitigation techniques and practices. He is presently Co-Investigator for the Magnetometer on the MESSENGER Discovery mission to Mercury, Principal Investigator on the Active Magnetosphere and Planetary Electrodynamics Response Experiment (AMPERE) based on magnetic field measurements from the Iridium satellites, and magnetics cleanliness lead for the Magnetospheric MultiScale (MMS) mission.

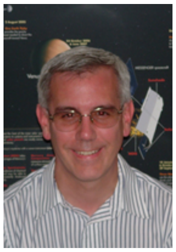

James McAdams is a Principal Staff engineer in the Mission Design, Guidance, and Control Group in the Space Department at the Johns Hopkins Applied Physics Laboratory. He received his B.S. and M.S.in Aeronautical and Astronautical Engineering from Purdue University. He has been the only Mission Design Lead Engineer for the MESSENGER Mercury Orbiter mission, and he was a key Mission Design team member of the Near Earth Asteroid Rendezvous (NEAR) through all development and operations phases. Jim also worked on the Galileo mission to Jupiter.

Dr. David Roth is senior physist in the Component Engineering group in the Space Department at the Johns Hopkins Applied Physics Laboratory. He received his B.S. in Physics and Mathematics from the Delaware State College, and his M.S. and Ph.D. in Physics from Clemson University. During his 13 years at APL he has contributed to all the major Space Department Programs as well as most of the instrument programs. Recently he has participated on the JEO/EJSM team as a radiation system engineer.